JOURNAL OF PROPULSION AND POWER
Vol. 12, No. 3, May–June 1996

Supersonic Shock/Turbulent Boundary-Layer Interaction on a Roughened Surface

George R. Inger*
Iowa State University, Ames, Iowa 50011

This article presents results from an exploratory study of roughness effects on shock-generated turbulent shock/boundary-layer interaction that specifically focuses on a small sand grain-type of roughness that falls within the framework of the law of the wall. With regard to the interaction zone itself, a triple-deck model is used to develop a theory of how such roughness alters the interactive flow physics. Some confirming experimental results are then given from a Mach 2.5 supersonic wind-tunnel study of both nonseparating and incipiently separating wedge shock-generated turbulent interactions on several roughened surfaces. These results show that even a small roughness significantly increases the upstream influence and enhances the onset of separation.

Nomenclature

B = law of wall parameter, Eq. (2)
C_f = skin friction coefficient, $2\tau_w/\rho_\infty U_\infty^2$
C_p = pressure coefficient, $2(p - p_\infty)/\rho_\infty U_\infty^2$
h = average roughness height
k = von Kármán's constant, Eq. (2)
L = reference length, Fig. 2
L_x, L_{yi} = interaction zone length scales, Fig. 2
l_u = upstream influence distance
M = Mach number
M_0' = $(dM_0/dy)_w$
N = power-law profile exponent, $u/u_e = \eta^N$
p = static pressure
Re_δ = Reynolds number, $\rho_\infty U_\infty \delta/\mu_\infty$
T = static temperature
U = streamwise velocity component
U_τ = friction velocity, $\sqrt{\tau_w/\rho_w}$
U^* = U/U_τ
U_∞ = freestream velocity
w = wake function, Eq. (2)
x, z = streamwise, lateral coordinates
y = distance normal to wall
y^* = $\rho_w U_\tau y/\mu_w$
β = $\sqrt{M_\infty^2 - 1}$
δ = boundary-layer thickness
δ^* = boundary-layer displacement thickness
ε = $R_{eL}^{-1/8}$, Fig. 2
η = y/δ_0
Θ^* = boundary-layer momentum thickness
λ = effective roughness parameter, Eq. (6)
μ = coefficient of viscosity
ν = μ/ρ
ρ = density
τ_w = wall shear stress

Subscripts
ADIAB = adiabatic wall value
e = local inviscid edge conditions of boundary layer
h = value pertaining to roughness
i = inner-layer edge
i.s. = incipient separation
LSL = laminar sublayer
SIP = shock impingement point
TEEP = trailing-edge expansion impingement point
w = conditions at wall surface
0 = noninteractive property
∞ = undisturbed freestream conditions

Presented as Paper 95-0229 at the AIAA 33rd Aerospace Sciences Meeting and Exhibit, Reno, NV, Jan. 9–12, 1995; received Feb. 1, 1995; revision received Nov. 30, 1995; accepted for publication Dec. 7, 1995.

*Professor of Aerospace Engineering, Department of Aerospace Engineering and Engineering Mechanics. Associate Fellow AIAA.

Introduction

A SOUND understanding of shock/turbulent boundary-layer interaction (SBLI) is important in the aerodynamical analysis of hypersonic vehicle flowfields and engine inlets. These interactions involve a strong viscous/inviscid interaction flow with a large local adverse pressure gradient that often provokes boundary-layer separation. Although many studies have been done on this problem, few have addressed a very important aspect that arises in practice: the effects of surface roughness such as the mesh of porous wall sections for boundary-layer control by suction, or overall distributed surface grittiness. These effects are particularly important at the large Reynolds numbers of full-scale aircraft where the thin boundary layers involved are subject to influence by even small roughness elements ($h/\delta << 1$).

All existing theoretical and computational tools for predicting SBLI assume a smooth wall with no provision for treating surface roughness effects. With regard to experimental data, a small body of studies has accumulated[1–3] which qualitatively show that roughness effects are indeed significant (see, e.g., Fig. 1). However, a more detailed assessment reveals that these studies collectively suffer a number of shortcomings and limitations, as follows:

1) References 1 and 3 do not involve roughness, but actually deal with protuberances $h/\delta > 1$, whose effects are often difficult to describe within the law of the wall/law of the wake framework so fundamental to turbulent boundary layers.[4]

2) They provide only general physical trends with little in the way of detailed boundary-layer profile and skin friction data that can serve for computational fluid dynamics (CFD) code validation (a recent improvement on this situation can be found in Ref. 3).

3) They offer no specific theoretical framework with which to understand and correlate the observed role of roughness in the SBLI zone.

4) The existing data are confined to the case of compression corner interactions; the companion (and equally important) problem of incident shock-generated interactions has yet to be studied.

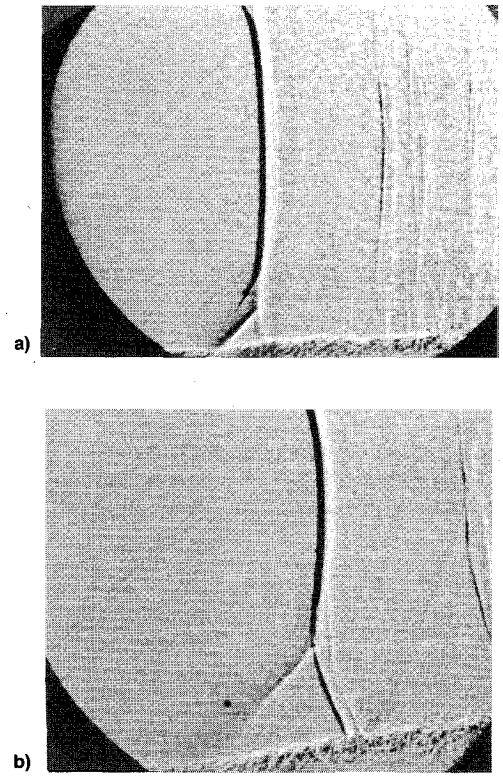

Fig. 1 Schlieren photographs showing wall-riblet roughness effect on a typical transonic SBLI: a) smooth wall and b) riblets on wall. (Photograph courtesy L. Squire, Cambridge University.)

This article addresses these issues for the case of steady adiabatic two-dimensional flow: it presents results from an exploratory theoretical and experimental study of roughness effects on shock-generated turbulent SBLI that specifically focuses on small ($h/\delta < 1$) subboundary-layer roughness. In particular, it deals with the classical three-dimensional sand grain-type of roughness that falls within the framework of the law of the wall/law of the wake. As regards the interaction zone itself, we use a triple-deck model as the conceptual basis to develop a preliminary theory of how such roughness alters the interactive flow physics. Following this, we present some confirming experimental results from a Mach 2.5 supersonic wind-tunnel study of both nonseparating and separating wedge shock-generated turbulent interactions on several roughened surfaces.

Theoretical Considerations

Incoming Boundary Layer

The law of the wall/law of the wake concept is adopted here to describe the incoming turbulent boundary layer ahead of the SBLI zone. With respect to the velocity profile properties of the smooth wall case, the main physical effects that small scale ($h/\delta < 1$), distributed sand grain-type roughness is known to have, fall into three regimes.[4] The first is the so-called hydraulically smooth regime, $h \leq y_{LSL}$ ($h^* \leq 11-12$), where the roughness is buried within the laminar (linear) sublayer and so has no sensible effect on the flow. The second is an intermediate, above-critical regime $11 \leq h^* \leq 70$, in which the roughness begins to have discernible effects on the flow in that it shifts $u^*(y^*)$ downward, thickens the boundary layer, and introduces a drag increase that reduces the velocity in the physical $u(y)$ profile. This last feature can be approximately modeled by the well-known power-law expression,[5]

$$u/u_e \approx (y/\delta)^N \tag{1}$$

where $N \sim \frac{1}{7}$ for smooth surfaces, but $\sim\frac{1}{5}$ to $\frac{1}{4}$ for rough ones. The third is the fully rough regime $h^* > 70$ (but, $h < \delta$), where the roughness is so big that it obliterates all vestiges of the laminar sublayer and imposes its own scale on the law of the wall region. This produces the viscosity-independent law of the wall profile that

$$u^* = B + (1/k)\ell n(y/h) + (\pi/k)w \tag{2}$$

where B depends on the roughness geometry and density, and where w remains negligibly affected by roughness provided $h/\delta < 1$. In view of its database, Eq. (2) will be taken to apply only above the maximum roughness crests.

Interaction Region

A second element of our theoretical framework is the triple-deck concept for the disturbance flow structure in the SBLI zone; a schematic illustration of this is given in Fig. 2 for the smooth wall case. This is used as a basis to develop a model of how roughness can alter the local interactive physics.

Consider an incoming supersonic turbulent δ_0 and Mach number profile $M_0(y)$ ahead of an SBLI zone (Fig. 2); then for nonseparating interactions, Lighthill showed in a classic paper[6] that l_u of the interaction depends very sensitively on $M_0(y)$, according to the general expression

$$\beta(l_u/\delta_0) = M_e^2 \int_{y_i/\delta_0}^{1} \left(\frac{1 - M_0^2}{M_0^2}\right) d\eta + \beta^2 \int_0^1 M_0^2\, d\eta \tag{3}$$

where $\eta = y/\delta_0$ and $y \leq y_i$ contains the linear portion of the Mach number profile. For smooth walls, Lighthill further showed that evaluation of the first integral by the mixed linear/power-law representation

$$M_0^2 \approx \{[M_0'(0)y]^{-2} + M_e^{-2}\eta^{-2N}\}^{-1} \tag{4a}$$

and evaluation of the second integral by the purely power-law approximation

$$M_0^2 \approx M_e^2 \eta^{2N} \tag{4b}$$

further yields from Eq. (3) the expression

$$\beta \frac{l_u}{\delta_0} \approx \underbrace{\left(\frac{4N}{1 - 4N^2}\right)\left[1 - \left(\frac{1 - 2N}{2}\right) M_e^2\right]}_{\text{middle deck}} + \underbrace{\left[\frac{M_e}{M_0'(0)\delta_0}\right]^2 \frac{1}{\eta_i}}_{\text{inner deck}} \tag{5}$$

where it is emphasized that the exponent N here pertains to smooth surfaces[5] (typically $\sim\frac{1}{7}$). Equation (5) indicates that the

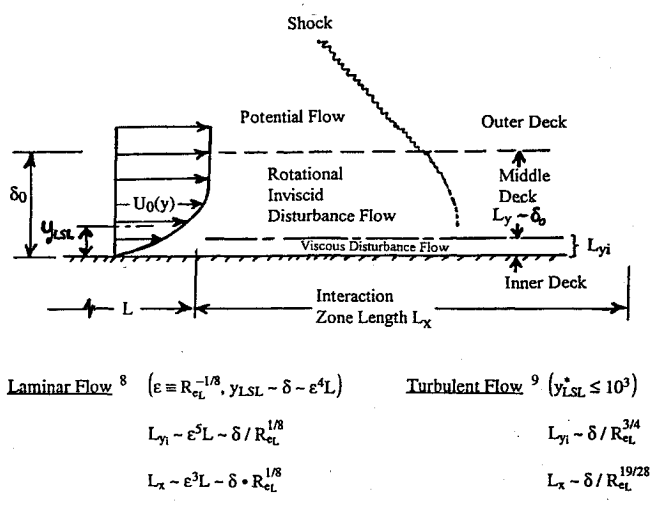

Fig. 2 Triple deck structure of a smooth wall SBLI zone (schematic).

upstream influence ratio l_u/δ_0 derives from two sources: 1) a Reynolds number-independent contribution from the profile shape across the middle deck, and 2) a Reynolds number-dependent contribution dominated by events in the inner deck adjacent to the wall {the factor $M_0'(0)\delta_0/M_e = C_f Re_{\delta 0}/[2(\mu_w/\mu_e)\sqrt{T_w/T_e}]$}, and inversely proportional to η_i (which in the smooth wall case is given by a further detailed analysis of the viscous inner deck flow[6]). Numerically, both contributions are of order unity, explaining the fact that $l_u \sim \delta_0$ is observed experimentally for such turbulent interactions.[7-9]

Turning now to interactions on a wall in the fully rough regime where $h^* \geq 70$, but still with $h/\delta < 1$, we would expect such roughness to wipe out the effects of laminar viscosity and the inner deck so as to replace the lower limit y_i on the first integral of Eq. (3), by a value directly proportional to, but above, the roughness height itself. In the first approximation we take this as $\eta_i \approx \lambda h/\delta \equiv \eta_h$, where λ is an empirical factor on the order of 2–3, and evaluate both integrals in Eq. (3) on the basis of Eq. (4b), with N now taking the value pertaining to a rough wall; this yields

$$\beta \frac{l_u}{\delta_0} \approx \underbrace{\left(\frac{4N}{1-4N^2}\right)\left[1-\left(\frac{1-2N}{2}\right)M_e^2\right]}_{F_m} + \underbrace{\left[M_e^2 - \left(\frac{\eta_h^{-2N}}{1-2N}\right)\right]\eta_h}_{F_h} \tag{6}$$

Comparing this with Eq. (5), it is seen that roughness increases the middle deck contribution F_m (because of the larger N), while replacing the viscous-dominated inner deck contribution by a direct roughness height effect function F_h that is of comparable or larger magnitude, especially at higher Mach numbers (see the typical values plotted in Fig. 3). The SBLI zone on a fully rough wall becomes effectively a double-decked rotational inviscid flow with a slip velocity at the bottom, which is proportional to the roughness height.

The foregoing implies that roughness has two main effects on the streamwise extent of the interaction: 1) by increasing δ_0 slightly, it likewise increases $l_u \sim \delta_0$; and 2) beyond this simple scaling, the aforementioned detailed roughness effect

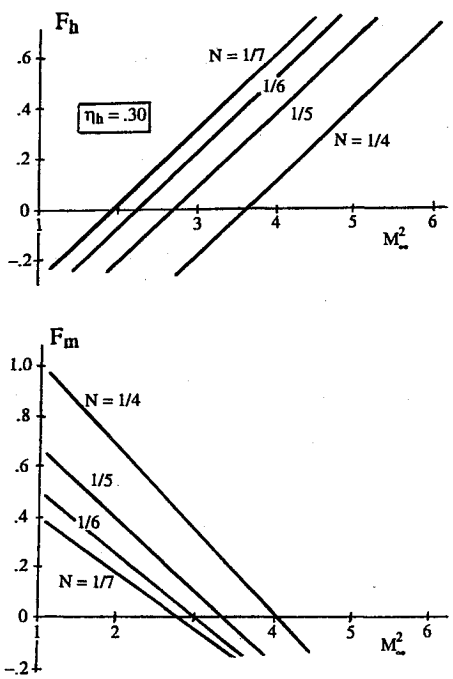

Fig. 3 Interaction roughness-effect functions.

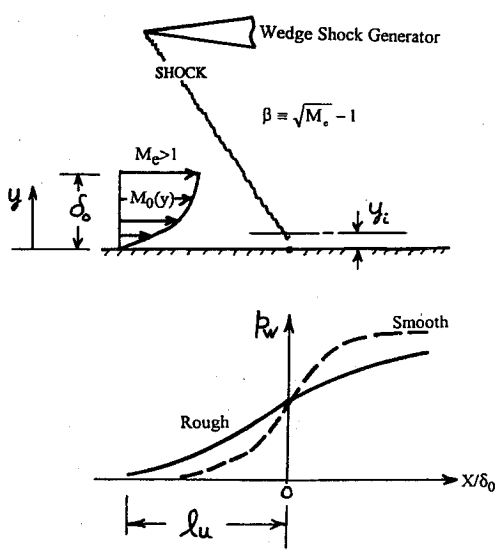

Fig. 4 Roughness effect on the interactive pressure rise (schematic).

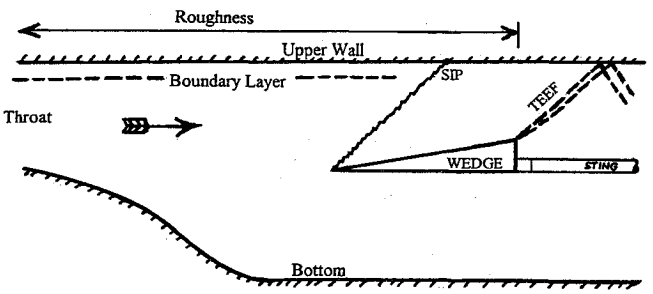

Fig. 5 Experimental arrangement for schlieren study of shock impingement on roughened upper wall (side view).

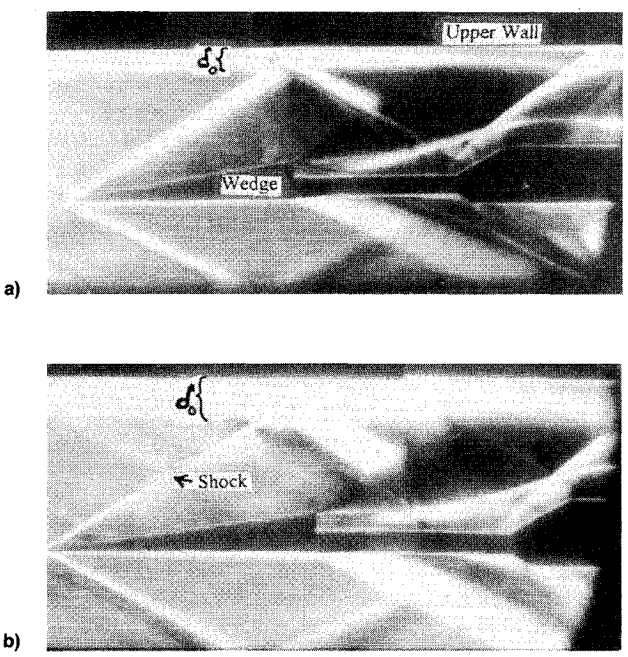

Fig. 6 Typical schlieren results showing the roughness effect on the SBLI zone. Eight-deg wedge: a) no wall roughness and b) maximum wall roughness.

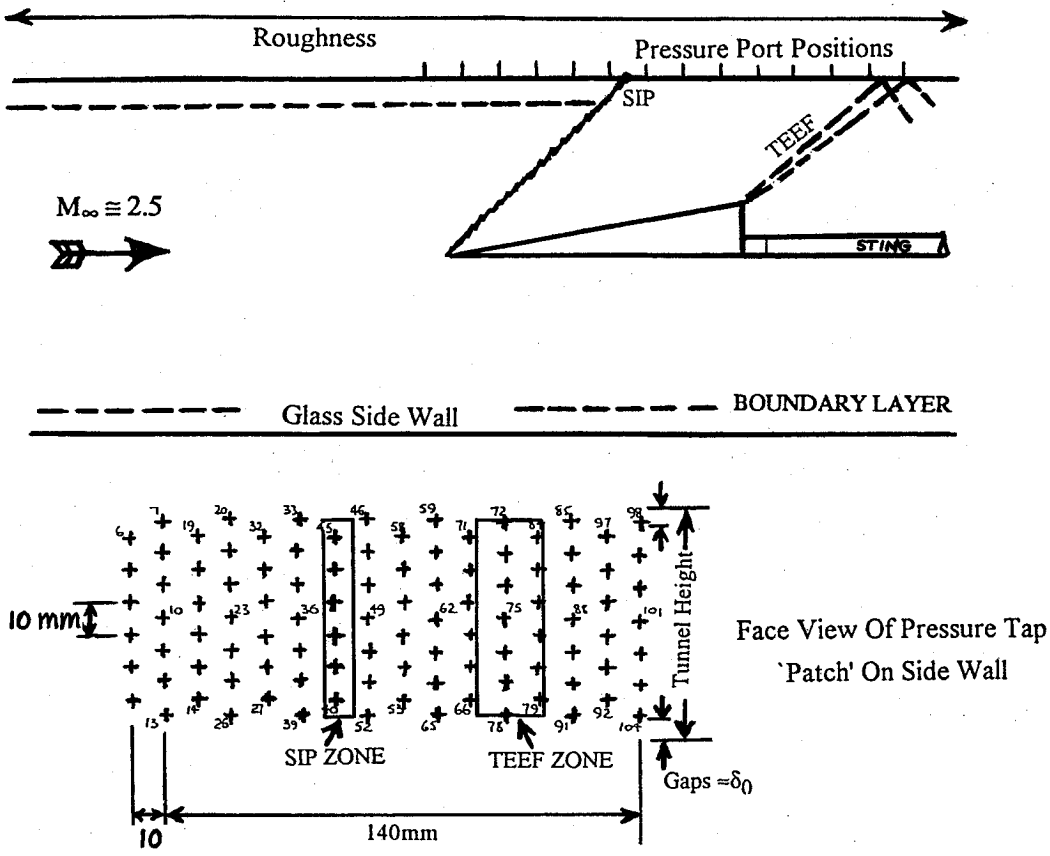

Fig. 7 Experimental arrangement for the pressure distribution measurements on the roughened side wall (plan view).

on the boundary-layer profile further increases l_u. This is schematically illustrated in Fig. 4 and will be corroborated by the experiments described next.

The foregoing can be carried further into an estimate of the roughness effect on incipient separation as well. If one does a Chapman-type order of magnitude analysis of this free interaction problem,[10] it can be shown[11] that the interactive pressure rise coefficient needed to first produce $C_f = 0$ in the interaction zone, is of order

$$C_{p_{i.s.}} \sim [\beta(l_u/\delta_0)]^{-1} \tag{7}$$

Since we have just seen that roughness increases l_u/δ_0, we conclude that it correspondingly reduces $C_{p_{i.s.}}$, and hastens the onset of separation in agreement with known experimental observations.[1-3]

Experimental Results

We next present some results from a pilot experimental study in a small supersonic wind tunnel, carried out under the author's supervision. The specific facility used was the 2.5 × 2.5 in. test section blow-down tunnel of the Cranfield University College of Aeronautics, having a 30-s steady test flow Mach number of 2.5 at a unit Reynolds number of 10^4/mm. This wind-tunnel facility has been used in many previous studies, and its general test section flow properties are well established. Although the detailed law of the wall structure in the wall boundary layers has not been documented, the $\delta_0 \cong 5.8$-mm-averaged smooth wall value observed by schlieren in the test section is consistent with a fully developed turbulent boundary layer over the available 1.3-ft streamwise distance from the throat at this Reynolds number. Furthermore, profile surveys have established the corresponding displacement and momentum thickness values $\delta_0^* = 0.2\delta_0$ and $\theta_0^* \cong 0.06\delta_0$, respectively, which are also typical of an equilibrium flat plate turbulent boundary layer.

A sting-mounted wedge shock generator was used; depending on the orientation of the wedge, several different tests were carried out with emphasis on discerning the relative influence of roughness compared to the smooth wall case.

Some qualitative studies by schlieren photography were first made of the wall roughness effect on the interactive wave patterns in the interaction zone, with the wedge-generated shock impinging on the upper test section wall as schematically illustrated in Fig. 5. Two different grades of sandpaper roughness were taped to the entire length of the upper wall, providing averaged roughness heights of $h/\delta \approx 0.06$ and 0.16, respectively. These heights correspond to 2.8- and 7.7-laminar sublayer thicknesses, respectively, at this Mach number assuming an adiabatic wall. Typical results for an 8-deg half-angle wedge shock incident on both the smooth and maximum rough walls are presented in Fig. 6, where the increased local boundary-layer thickness and upstream influence of the interaction in the presence of roughness can be seen. The specific values of δ_0 observed in this case ranged from the smooth wall value of 5.8 mm to values of 6.5 and 8 mm, respectively, for the aforementioned two roughness heights. Note in this regard that a detailed profile survey of these roughened incoming boundary layers was deemed outside the scope of this exploratory study, and is delegated to a follow-on investigation in a more commodious facility should the present findings warrant it.

A second series of measurements was then made to obtain interactive surface pressure distributions. To avoid corner and side-wall effects, these were done by rotating the wedge shock generator 90 deg about its sting axis to a vertical position such that its shock impinged on the side wall, as illustrated in Fig. 7. The wedge was not full span across the test section height to alleviate the effects of glancing interaction between the oblique shock and the tunnel side walls. A patch of the resulting SBLI zone on the side wall (less in width than the tunnel height by approximately twice the wall boundary-layer thickness) was instrumented with a matrix of pressure taps

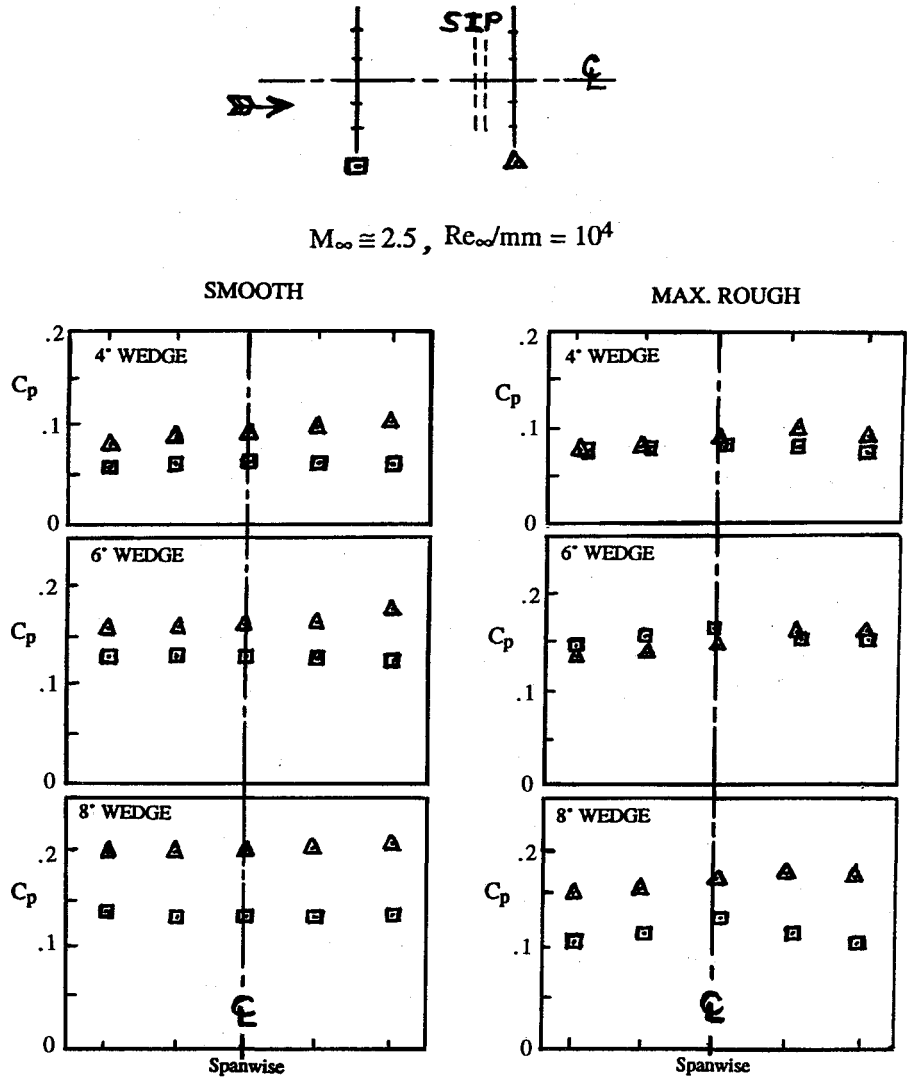

Fig. 8 Spanwise wall pressure survey data for smooth and rough walls.

clear through the roughness (also shown in Fig. 7), connected by flexible plastic tubing to kulite transducers (further details of the usual scanivalve output-digitalization equipment used are omitted). The typical uncertainty in these pressure measurements is approximately 3%. The interactions associated with five different wedge half-angles (4, 5, 6, 7, and 8 deg) were studied on smooth and roughened side-wall surfaces, with emphasis on discerning the relative effects of roughness for a given incident shock strength. Note that the 8-deg wedge interaction is expected to be on the threshold of incipient separation for a turbulent boundary layer along a smooth wall under the present test conditions,[7] and this indeed appeared to be the case.

To assess the spanwise uniformity aspect of the data, we present in Fig. 8 the measured lateral pressure variations (perpendicular to the streamwise direction) at two different streamwise stations along the SBLI zone: one in the upstream influence region upstream of the shock impingement line, and the other in a region slightly downstream of shock impingement. This is done for both the smooth and maximum rough surface conditions at each of three different wedge angles. Inspection of these data yields two major conclusions. First, aside from a few irregularities, a reasonably constant spanwise wall pressure field was obtained in the center half of the interaction zone both upstream and downstream of shock impingement for all of the conditions investigated; the maximum spanwise pressure variations from the centerline value ranged from 6 to 14% for both smooth and rough walls. Given the aforementioned absence of side plates, this is sufficiently spanwise-uniform for the present purposes. Second, the presence of roughness, although certainly affecting the pressure levels, did not sensibly affect this spanwise uniformity. In what follows we use a five-station spanwise average astride the centerline at each streamwise station to obtain the streamwise pressure distributions.

A summary of the streamwise interactive pressure distributions so obtained for each of the five wedge angles is presented in Fig. 9, plotted as C_p vs the nondimensional distance x/δ_0, where x is the distance relative to the inviscid shock impingement station and δ_0 is the boundary-layer thickness corresponding to the wall roughness involved (this choice of abscissa absorbs that part of the roughness effect associated with a simple scaling with δ_0). For each wedge angle (incident shock strength), the results for both the smooth and the two roughened wall conditions are shown to enable direct comparison. These data exhibit the expected three-dimensional effects associated with lateral bleed around the finite span incident shock, namely, a lower than inviscid maximum pressure level[12] (in the present case 20–25% lower), followed by a gradual pressure drop, which here is further enhanced downstream by impingement on the wall of the wedge trailing-edge expansion fan. Nevertheless, judging by the unseparated flow data for the small (4–6 deg) wedge angles combined with the previous observations about the spanwise pressure survey, it appears that the roughness did not significantly alter the degree of these three-dimensional effects. At least up to the region of

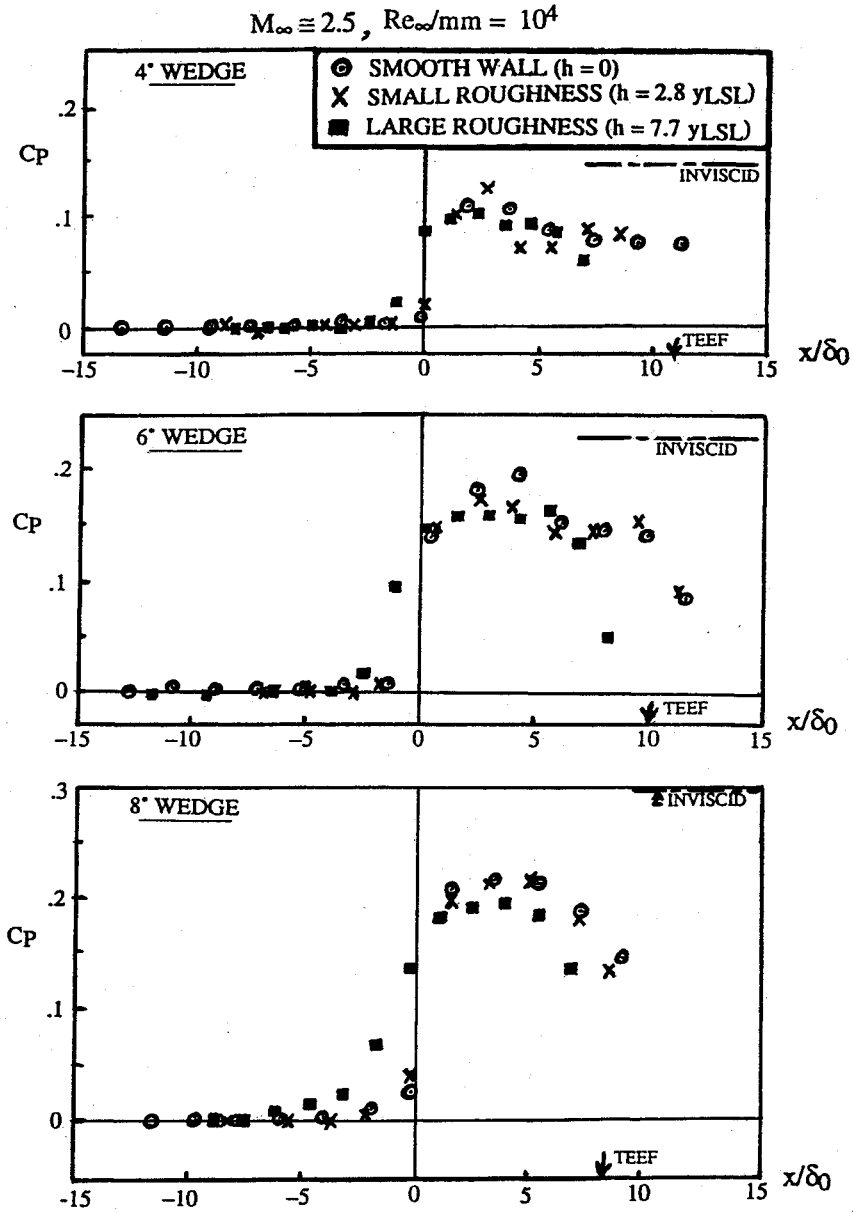

Fig. 9 Streamwise pressure distribution along the interaction zone.

maximum pressure, the difference between the rough and smooth may therefore be attributed to purely the effects of roughness per se.

Focusing on Fig. 9, as regards the relative effects of roughness on the interactive pressure distributions, it can be seen that the larger roughness $h \cong 7.7y_{LSL}$ appreciably increased the upstream influence ratio l_u/δ_0, especially at the larger wedge angles. Moreover, such enhanced upstream pressure rise implies an earlier onset of incipient separation, see especially the 8-deg wedge data. The aforementioned features are both in qualitative agreement with the previous predictions of our theoretical model for a roughness-dominated interaction. Turning to the data for the small roughness $h \cong 2.8y_{LSL}$, it is seen in this case that roughness had only a very small effect at all wedge angles. This result is also consistent with our combined law of the wall/triple-deck interaction model, which predicts a negligible explicit effect of laminar sublayer-scale roughness when the interaction is dominated by the outer power-law profile region of the boundary layer as is the case in a turbulent flow.

Another less pronounced, but noticeable effect of the layer roughness that can be observed in Fig. 9, is a moderate reduction in the maximum pressure rise relative to the smooth wall case that occurs at the larger wedge angles. Assuming that this is not attributable to an influence of roughness on the three-dimensional effects, we conjecture that such an observation could be explained by the reduced dynamic pressure deep in the boundary layer associated with the roughness-induced momentum under conditions of slight flow separation.

Concluding Remarks: Future Work

The present study has established that even subboundary-layer distributed (sand grain-type) roughness can significantly alter the flow in an impinging shock/turbulent boundary-layer interaction zone, provided the roughness is well above the laminar sublayer. Moreover, we have constructed a preliminary theory of this that qualitatively agrees with the data in showing that even small roughness increases the upstream influence of the interaction and enhances the onset of separation. These findings are deemed sufficiently interesting to warrant more detailed future study.

Acknowledgments

The author is indebted to the British Science and Engineering Council for financial support and to John Stollery of Cranfield University, England, UK, for many helpful discussions.

References

[1]Holden, M. S., "Studies of Boundary Layer Transition and Surface Roughness Effects in Hypersonic Flow," Air Force Office of Scientific Research Rept. 6430-A-5, Washington, DC, Oct. 1983.

[2]Disimile, P. J., and Scaggs, N. E., "Wedge-Induced Turbulent Boundary Layer Separation on a Roughened Surface at Mach 6.0," *Journal of Spacecraft and Rockets*, Vol. 28, No. 6, 1991, pp. 634–645.

[3]Babinsky, H., "A Study of Roughness in Turbulent Hypersonic Boundary Layers," Ph.D. Dissertation, Cranfield Univ., Cranfield, England, UK, Dec. 1993.

[4]White, F. M., *Viscous Flow Theory*, 2nd ed., McGraw–Hill, New York, 1992.

[5]Schlichting, H., *Boundary Layer Theory*, 7th ed., McGraw–Hill, New York, 1968.

[6]Lighthill, M. J., "On Boundary Layers and Upstream Influence; II. Supersonic Flow Without Separation," *Proceedings of the Royal Society of London, Series A: Mathematical and Physical Sciences*, Vol. 217, 1953, pp. 478–507.

[7]Kuehn, D. M., "Experimental Investigation of the Pressure Rise for Incipient Separation of Turbulent Boundary Layers in Two Dimensional Supersonic Flow," NASA Memo 1-21-59A, Feb. 1959.

[8]Stewartson, K., "Multistructural Boundary Layers on Flat Plates and Related Bodies," *Advances in Applied Mechanics*, Vol. 14, Academic, New York, 1974.

[9]Inger, G. R., "Nonasymptotic Theory of Unseparated Turbulent Boundary Layer Interaction," *Numerical and Physical Aspects of Aerodynamic Flows*, edited by T. Cebeci, Springer–Verlag, New York, 1983.

[10]Lewis, J. F., Kubota, T., and Lees, L., "Experimental Investigation of Supersonic Laminar Two Dimensional Boundary Layer Separation in a Compression Corner," *AIAA Journal*, Vol. 6, No. 1, 1968, pp. 7–15.

[11]Inger, G. R., "Similitude Properties of High Speed Laminar and Turbulent Boundary Layer Separation," *AIAA Journal*, Vol. 15, No. 5, 1977, pp. 619–623.

[12]Reda, D. C., and Murphy, J. D., "Shock Wave/Turbulent Boundary Layer Interactions in Rectangular Channels," *AIAA Journal*, Vol. 11, No. 2, 1973, pp. 139–141.